Correlation based modelling and separation of geomagnetic field components

Matthias Holschneider[1], Vincent Lesur[2], Stefan Mauerberger[1], and Julien Baerenzung[1]

[1]Institut für Mathematik, Universität Potsdam
[2]Institut de physique du globe de Paris (IPGP)

January 8, 2016

Abstract

We introduce a technique for the modeling and separation of geomagnetic field components that is based on an analysis of their correlation structures alone. The inversion is based on a Bayesian formulation, which allows the computation of uncertainties. The technique allows the incorporation of complex measurement geometries like observatory data in a simple way. We show how our technique is linked to other well known inversion techniques. A case study based on observational data is given.

1 Introduction

Modelling the Earth magnetic field is an essential step towards understanding the dynamic processes at work in the Earth's outer core. There, is generated the *core field* that dominates the observed magnetic field at the Earth's surface. Its rapid temporal variations in strength and direction, have been the focus of most of the modelling work over the last ten years. However, these variations remain poorly described and understood; they can be revealed only if contributions from the lithosphere, ionosphere, magnetosphere and other weaker signals are accounted for. The separation of these different contributions to magnetic field measurements remains one of the main challenges in building magnetic field models.

Traditionally, models of the Earth's core magnetic field have been built from observatory data. This carries the challenge of dealing with the sparseness of the observatory distribution as well as handling the unknown magnetic field generated locally by the rocks surrounding the observatories. However, models have been built this way, sometimes using also repeat station or other ground survey data, catching the main behaviour of the field (see Gillet et al. (2009) for a review). In such models, contributions of the external fields have been mostly ignored.

The Magsat mission was the first satellite mission providing vector magnetic data on global scales. The mission was very short, with only around 6 months of data. Nonetheless magnetic field models were derived by least squares using a system of representation based on spherical harmonics (e.g. Langel et al. (1980)). The models typically included the main magnetic field and its secular variation, sometimes a large-scale external field with its induced counterpart, and also, due to the relatively low altitude of the satellite orbits, the lithospheric field. The separation of the internal and external parts of the field was essentially based on strong smoothness assumptions on the internal field temporal behaviour, and a representation of the external fields using only the first spherical harmonic degrees.

Since then, all models of the magnetic field derived from satellite data are relying on the same technique. Naturally, due to the significant increase of data quality during the Oersted and Champ satellite missions, the temporal resolution of the internal field models has been significantly improved. Technically the most advanced models are using order 6 B-splines functions in time – e.g. the CHAOS (Olsen et al. (2006, 2009, 2010); Olsen et al. (2014)) and GRIMM (Lesur et al. (2008, 2010); Mandea et al. (2012); Lesur et al. (2015)) series of models, with nodes 6 months apart. Other approaches exist, like Sabaka et al. (2015) or Chulliat and Maus (2014). Nonetheless, smoothing constraints have to be applied to avoid leakage of the external field inside the internal field model. However it is clear that the external field parameterisation, as well as its induced counterpart is not able to explain the full complexity of the ionospheric and magnetospheric field behaviours. Furthermore, some types of signals – e.g. tidal signals, are generally not accounted for in the parameterisation. As a result, there are remaining signals in the residuals of the least squares fit to the data, which are necessarily correlated in space and time. It is therefore a major challenge to statistically describe the prior covariance matrix of the residuals, aside form the fact that, due to the correlations, this matrix is full and cannot be easily handled on modern computers as soon as the number of data exceed few ten thousands. Without proper prior covariance matrix for the data, there is no hope to have a realistic estimate of the posterior covariance matrix of the magnetic field model.

Indeed it has been very soon recognised that variances of the model parameters – i.e. the Gauss coefficients, are heavily under-estimated. There has been a significant pressure from the user community – e.g. for using magnetic field models in assimilation framework or for industrial applications, to provide more information on the accuracy and reliability of the magnetic field models. Some models are provided with this information – e.g. (Lesur et al., 2010). The problem of the underestimation of the parameter variances and co-variances has also been independently studied by Lowes and Olsen (2004). When models are derived from observatory data (e.g. Wardinski and Lesur (2012)), the difficulties are the same. In Gillet et al. (2013) attempts are made to control better the effect of the regularisation on the Gauss coefficient resolutions and accuracies, but the difficulty associated with the separation of internal and external contributions remains unresolved.

In short, when using the spherical harmonic representation of the magnetic field contributions, the separation of the external and internal fields requires an under-parameterisation of these contributions that precludes the derivation of a realistic posterior covariance matrix of the model. A possible way to circumvent this problem is to drop the usual spherical harmonic representation, and base the separation of external and internal field on other principles. In this paper we propose therefore to use a correlation-based technique, similar to the collocation methods in gravity, where harmonic spline representation is underpinning the calculation of these correlations and enable the separation of the external and internal contributions.

Harmonic splines have been introduced for magnetic field modelling by Shure et al. (1982). They have been used mainly for interpolation purpose (e.g. Wessel and Becker (2008)) or to model the field on regional scale (Geese et al., 2010). The *representer* approach described in Parker (1994) is a related technique that has been used mainly for lithospheric field studies (Whaler and Langel, 1996; Whaler and Purucker, 2005). Another closely related technique has been proposed in Constable et al. (1993) and Jackson et al. (2007) to model the core field under topologic constraints. It has also been applied to the lithospheric field (Stockmann et al., 2009). To our knowledge harmonic splines have never been used to model together internal and external magnetic fields. Mathematically, they are defined in a reproducing kernel Hilbert space, and the way the scalar product is defined in this space allows building harmonic splines that have specific characteristics. In particular, defining the behaviour of the spectra as a function of the wavelength at the core-mantle boundary, or at high altitude, allows separating the contribution of the internal and external sources to the magnetic field.

The aim of this paper is mainly to describe the mathematical framework of this correlation-based technique for modelling the Earth's magnetic field. After a short general first section, we construct explicit correlation kernels for all field components of the magnetic field. We show, how this formalism may be used to separate the various field components and demonstrate it on a data set made of magnetic field observatory monthly means (Macmillan and Olsen, 2013).

2 Correlation based modelling of geomagnetic fields

Usually, magnetic field models $\mathbf{B}$ are defined through the gradient of a potential

$$\mathbf{B}(x) = -\nabla\Phi(x) \; . \tag{1}$$

The potential is usually given in terms of a collection of basis functions F_n and parametrized by coefficients α_n:

$$\Phi(x) = \sum \alpha_n \, F_n(x) \; . \tag{2}$$

Typically, one uses spherical harmonics. Due to completeness reasons the sum in Equation 2 is a priori infinite, which leads to an underdetermined system. To restore uniqueness, regularisation is applied. It can be shown that there are effective basis functions for a regularisation based on generalised geomagnetic energies, such that this *unique* solution can also be found in terms of a finite expansion (Parker, 1994). These basis functions are the so-called reproducing kernels of the smoothing spline. In that case the sum of basis functions F_n contains as many terms as we have observations.

In the following, we propose an approach which does not use a parametrisation of the form outlined above, but is closely related to harmonic splines. The modelling is purely based on correlation structures of the magnetic field and its observables. We present a coherent formulation that does not appeal to a particular parametrisation, but focuses on the physics of the problem.

Suppose, an a priori correlation structure of the magnetic potential Φ is known. This correlation structure includes all our physical knowledge and can be used to estimate the magnetic field from measurements. The correlation is determined by a correlation kernel

$$K(x, y) = \mathbb{E}\Big[\Big(\Phi(x) - \overline{\Phi(x)}\Big)\Big(\Phi(y) - \overline{\Phi(y)}\Big)\Big] \; , \tag{3}$$

where $\mathbb{E}[\cdot]$ denotes the calculation of the expectation and $\overline{\Phi} = \mathbb{E}[\Phi]$ refers to the potential's mean value. The correlation kernel incorporates knowledge of the order of magnitude of the magnetic fields (i.e. the diagonal part of K) as well as the typical length scale over which the fields are correlated. It may even contain information about the geometry of the source distributions. In this paper however we will not consider this aspect.

Let us assume that the magnetic field is caused by four source regions: the core, the lithosphere, the ionosphere and the magnetosphere. Then, the potential Φ consists of four parts:

$$\Phi = \Phi_C + \Phi_L + \Phi_I + \Phi_M \tag{4}$$

Subscripts C, L, I and M refer to core, lithosphere, ionosphere and magnetosphere, respectively. Neglecting for now all kinds of induction effects, we can assume these component sources are uncorrelated. Under this assumption, the correlation structure of Φ is simply the sum of the correlations of its components:

$$K(x, y) = \alpha_C^2 K_C(x, y) + \alpha_L^2 K_L(x, y) + \alpha_I^2 K_I(x, y) + \alpha_M^2 K_M(x, y) \; . \tag{5}$$

The amplitude factors α^2 could in principle be absorbed into each of the kernel. However it is very convenient to leave them that way so that the a priori amplitudes of each of the components can be adjusted easily without changing the shape of the correlation of the component.

Since these components show distinct statistical characteristics with respect to strength and correlation length, a statistical procedure to separate them becomes available.

We use Bayesian analysis to obtain, from the prior knowledge imbedded in the correlation kernel and from vector magnetic field observations, information about these components.

Away from its sources, the magnetic field is the negative gradient of its potential and it can be observed at a series of N observation points:

$$\mathbf{B}(x_k) = -\nabla\Phi(x_k) \quad \text{for} \quad k = 1, \cdots, N \; . \tag{6}$$

The correlation structure of the magnetic potential implies the correlation of the magnetic field:

$$\begin{aligned} &\mathbb{E}\left[\left(\mathbf{B}(x) - \overline{\mathbf{B}(x)}\right)\left(\mathbf{B}(y) - \overline{\mathbf{B}(y)}\right)^t\right] = \\ &= \mathbb{E}\left[\left(\nabla\Phi(x) - \nabla\overline{\Phi(x)}\right)\left(\nabla\Phi(y) - \nabla\overline{\Phi(y)}\right)^t\right] = \nabla K(x,y)\nabla^t \; , \end{aligned} \tag{7}$$

where $K(x, y)$ refers to the kernel defined in equation 5. We use the following convention: A nabla operator on the left acts on the kernel's first argument whereas the second argument of the kernel is subject to the gradient on the right hand side. The superscript t indicates the transpose.

To obtain information on the magnetic field we need to compute the field's conditional probability given the set of N magnetic vector field observations. For example, the information about the core component of the potential we obtain from the observations is

$$\mathbb{P}(\Phi_C | \{\mathbf{B}(x_k)\}_{k=1,N}) \; , \tag{8}$$

i.e. the probability to have a potential Φ_C knowing the $3N$ observables $\mathbf{B}(x_k)$ with $k = 1, \ldots, N$. Note that each vector component of $\mathbf{B}$ is an observable in its own. To give another example, we can express our knowledge about the Gauss coefficients $g_{C;\ell,m}$ of the main field in the same way

$$\mathbb{P}(g_{C;\ell,m} | \{\mathbf{B}(x_k)\}_{k=1,N}) \; . \tag{9}$$

Assume the magnetic potential Φ to be the realisation of a Gaussian random field. Then, since the Gauss coefficients depend linearly on the potential, these conditional probabilities are again Gaussian distributed and fully determined by their mean and covariance.

The computation of those means and covariances is based on the following theorem. Let $\mathbf{m}$ and $\mathbf{B}$ be random vectors such that their joint $V = [\mathbf{m}^t, \mathbf{B}^t]^t$ is a multivariate Gaussian random vector. Then, $\mathbf{m}$ and $\mathbf{B}$ are Gaussian random variables, as well, and determined by

$$\mathbb{E}(\mathbf{m}) = \overline{\mathbf{m}} \qquad \text{and} \qquad \mathbb{E}(\mathbf{B}) = \overline{\mathbf{B}} \tag{10}$$

for their means, and

$$\begin{array}{rclcl}\mathbb{E}[(\mathbf{m}-\overline{\mathbf{m}})(\mathbf{m}-\overline{\mathbf{m}})^t] &=& \mathrm{Cov}[\mathbf{m},\mathbf{m}] &=& \Sigma_{\mathbf{mm}} \\ \mathbb{E}\big[(\mathbf{B}-\overline{\mathbf{B}})(\mathbf{B}-\overline{\mathbf{B}})^t\big] &=& \mathrm{Cov}[\mathbf{B},\mathbf{B}] &=& \Sigma_{\mathbf{BB}} \\ \mathbb{E}\big[(\mathbf{m}-\overline{\mathbf{m}})(\mathbf{B}-\overline{\mathbf{B}})^t\big] &=& \mathrm{Cov}[\mathbf{m},\mathbf{B}] &=& \Sigma_{\mathbf{mB}} \quad ,\end{array} \tag{11}$$

for their correlations. The conditional distribution for $\mathbf{m}$, given the observed magnetic field $\tilde{\mathbf{B}}$ – i.e. we observed that the random variable $\mathbf{B}$ takes the actual value $\tilde{\mathbf{B}}$, is again a Gaussian distribution and is therefore fully determined by its mean and covariance, which may be computed by standard theorems on multivariate Gaussians:

$$\begin{aligned}\overline{\mathbf{m}}_{|\tilde{\mathbf{B}}} &= \overline{\mathbf{m}} + \Sigma_{\mathbf{mB}}\Sigma_{\mathbf{BB}}^{-1}(\tilde{\mathbf{B}}-\overline{\mathbf{B}}) \\ \Sigma_{\mathbf{mm}|\tilde{\mathbf{B}}} &= \Sigma_{\mathbf{mm}} - \Sigma_{\mathbf{mB}}\Sigma_{\mathbf{BB}}^{-1}\Sigma_{\mathbf{mB}}^{t},\end{aligned} \tag{12}$$

where $\overline{\mathbf{m}}_{|\tilde{\mathbf{B}}}$ and $\Sigma_{\mathbf{mm}|\tilde{\mathbf{B}}}$ are the posterior mean and covariance of $\mathbf{m}$ knowing $\tilde{\mathbf{B}}$.

All the information about $\mathbf{m}$, as a Gaussian model of the field (e.g. the Gauss core field coefficients or core field snapshot values), can be obtained from observations $\tilde{\mathbf{B}}$ that depend linearly on the magnetic potential (e.g. a finite collection of field measurements which are the gradients of Φ at some points) from the Bayesian posterior distribution defined through equation 12.

3 Explicit correlation structures for the magnetic potential

In this section we propose a family of correlation structures based on the assumption that the Gauss coefficients describing a magnetic potential are uncorrelated on a sphere of given radius. We start with potentials for fields of internal origin and then introduce the relations for fields of external origin. The link to geomagnetic norms is also described.

3.1 Correlation structures for internal potentials

Suppose that Φ is a potential function outside some sphere of radius R

$$\Delta\Phi(x) = 0 \qquad\qquad |x| > R\,. \tag{13}$$

Like any other potential, Φ can be calculated everywhere outside its source region from its value on the surface of the sphere S_R of radius R. This is done using the (exterior) Poisson kernel $P(x,\zeta)$ given by:

$$\begin{aligned}P(x,\zeta) &= \frac{|x|^2-1}{|x-\zeta|^3} = & |x| &> 1 \\ &= \sum_{\ell,m}\frac{2\ell+1}{4\pi|x|^{\ell+1}}Y_{\ell,m}(\hat{x})Y_{\ell,m}(\zeta) & \hat{x} &= \frac{x}{|x|}\ ,\end{aligned} \tag{14}$$

where ζ is a vector on the unit sphere in direction θ, ϕ, and the Schmidt normalised spherical harmonics $Y_{\ell,m}(\theta, \phi)$ are written $Y_{\ell,m}(\zeta)$. The potential outside the sphere of radius R is then:

$$\Phi(x) = \int_{S_1} P(x/R, \zeta)\Phi(R\zeta)\mathrm{d}\Omega_1(\zeta) \tag{15}$$

$$= \int\limits_0^{2\pi}\int\limits_0^{\pi} P({}^x\!/_R, \theta, \phi)\, \Phi(R, \theta, \phi) \sin(\theta)\, \mathrm{d}\theta\, \mathrm{d}\phi \;. \tag{16}$$

It follows that if the correlation structure of the potential Φ on the sphere S_R is known, it is possible to calculate it everywhere outside the sphere. Lets assume that on the sphere S_R:

$$\mathbb{E}[\Phi] = 0\,, \qquad\qquad \mathbb{E}[\Phi(R\zeta)\, \Phi(R\eta)] = k(\zeta, \eta)\;, \tag{17}$$

where η is another vector on the unit sphere. Then the correlation outside the sphere is:

$$\begin{aligned}[\Phi(x)\Phi(y)] &=: K(x, y) \\ &= \int_{S_1}\int_{S_1} P({}^x\!/_R, \zeta)\, k(\zeta, \eta) P({}^y\!/_R, \eta)\, \mathrm{d}\Omega_1(\zeta)\, \mathrm{d}\Omega_1(\eta)\;.\end{aligned} \tag{18}$$

It remains to define a correlation $k(\zeta, \eta)$ for the magnetic potential on the sphere S_R. For this we consider the Gauss coefficients of the magnetic potential:

$$g_{\ell,m} = \frac{2\ell + 1}{4\pi R} \int_{S_1} Y_{\ell,m}(\zeta)\Phi(R\zeta)d\Omega_1(\zeta)\;. \tag{19}$$

The potential on the sphere of S_R is therefore:

$$\Phi(R\zeta) = R \sum_{\ell,m} g_{\ell,m} Y_{\ell,m}(\zeta)\;. \tag{20}$$

Assuming a correlation structure on the sphere S_R defined in terms of the degree variance λ_ℓ^2 of the Gauss coefficients:

$$\mathbb{E}[g_{\ell,m}] = 0\;, \qquad\qquad \mathbb{E}[g_{\ell,m}\, g_{\ell',m'}] = \lambda_\ell^2\, \delta_{\ell,\ell'}\, \delta_{m,m'}\;, \tag{21}$$

it leads through equations 17 and 20 to the correlation function $k(\zeta, \eta)$ equal to:

$$k(\zeta, \eta) = R^2 \sum_{\ell,m} \lambda_\ell^2 Y_{\ell,m}(\zeta) Y_{\ell,m}(\eta)\;. \tag{22}$$

At any two points outside the sphere S_R the correlation of the magnetic potential defined in equation 18 is therefore:

$$\mathbb{E}\left[\Phi(x)\, \Phi(y)\right] = R^2 \sum_{\ell,m} \lambda_\ell^2\, Y_{\ell,m}(\hat{x})\, Y_{\ell,m}(\hat{y}) \left(\tfrac{R^2}{|x||y|}\right)^{\ell+1} \tag{23}$$

$$= R^2 \sum_{\ell} \lambda_\ell^2\, P_\ell(\hat{x} \cdot \hat{y}) \left(\tfrac{R^2}{|x||y|}\right)^{\ell+1} \;. \tag{24}$$

In Section 4 we show how to derive simple analytic expressions for the correlation functions $K(x, y)$.

3.2 Interior to exterior mapping

We consider now the magnetic potential Φ inside a sphere of radius R.

$$\Delta\Phi(x) = 0\,, \qquad\qquad |x| < R\,. \tag{25}$$

Using the (interior) Poisson kernel $P(x, \zeta)$:

$$P(x,\zeta) = \sum_{\ell,m} \frac{(2\ell+1)|x|^\ell}{4\pi} Y_{\ell,m}(\hat{x}) Y_{\ell,m}(\zeta)\,, \qquad |x| < 1,\ \hat{x} = \tfrac{x}{|x|}\,, \tag{26}$$

we immediately obtain the equivalent of equation 23 for any point inside the sphere S_R:

$$\mathbb{E}[\Phi(x)\Phi(y)] = R^2 \sum_\ell \lambda_\ell^2\, P_\ell(\hat{x}\cdot\hat{y}) \left(\frac{|x||y|}{R^2}\right)^\ell \quad . \tag{27}$$

Hereinafter we call $K_E(x, y)$ (resp. $K_I(x, y)$) the correlation structure for potential of external (resp. internal) origin and define the position in space of $\tilde{x}$, the mirror image of x relative to the sphere S_R:

$$\tilde{x} = \frac{xR^2}{|x|^2} \quad . \tag{28}$$

It follows that:

$$K_E(x,y) = \frac{|\tilde{x}||\tilde{y}|}{R^2} K_I(\tilde{x},\tilde{y}) \quad . \tag{29}$$

On S_R the correlations K_E and K_I coincide.

3.3 Links with generalised geomagnetic energies

The order of magnitude of fields is measured by generalized geomagnetic norms or energies. In this section we show how this concept fits to our correlation structures. Let us introduce the vector of Gauss coefficients which is denoted by $\mathbf{g} = [g_{\ell,m}]_{\{\ell,m\}}$ for all degrees ℓ and orders m. For the Gauss coefficients a covariance matrix $\Sigma_{\mathbf{gg}}$ can be defined by considering Equation 21. Clearly, $\Sigma_{\mathbf{gg}}$ is diagonal.

The degree variance λ_ℓ^2 associated with the Gauss coefficients $g_{\ell,m}$ is independent of the order m as is expected for an isotropic correlation structure. Gauss coefficients are zero mean Gaussian random variables with probability density distribution

$$\mathrm{p}(\mathbf{g}) \propto e^{-\frac{1}{2}\Gamma[\mathbf{g}]} \tag{30}$$

where $\Gamma[\mathbf{g}]$ refers to a quadratic form. $\Gamma[\mathbf{g}]$ is equivalent to a so called generalized energy and is given by

$$\Gamma[\mathbf{g}] = \mathbf{g}^t \cdot \Sigma_{\mathbf{gg}}^{-1} \cdot \mathbf{g} = [g_{\ell,m}]^t_{\{\ell,m\}} \cdot \Sigma_{\mathbf{gg}}^{-1} \cdot [g_{\ell,m}]_{\{\ell,m\}} = \sum_{\ell,m} \frac{|g_{\ell,m}|^2}{\lambda_\ell^2} \tag{31}$$

depending on the choice of λ_ℓ. Let us introduce a scalar product based on the spatial average value of the magnetic potential over the sphere S_R

$$\langle \Phi_1, \Phi_2 \rangle = \frac{1}{4\pi R^2} \int_{S_R} \Phi_1(x)\, \Phi_2(x)\, \mathrm{d}\Omega_R(x) \tag{32}$$

$$= \frac{1}{4\pi} \int_{S_1} \Phi_1(R\zeta)\, \Phi_2(R\zeta)\, d\Omega_1(\zeta)\ . \tag{33}$$

The generalized energy of a field Φ with Gauss coefficients $\mathbf{g}$ can then be written using an operator Ξ as follows

$$\Gamma[\Phi] = \Gamma[\Phi, \Phi] = \langle \Phi, \Xi\Phi \rangle = \langle \Xi^{1/2}\Phi, \Xi^{1/2}\Phi \rangle = \Gamma[\mathbf{g}] \quad . \tag{34}$$

Such an operator always exists since the energy is a positive definite quadratic form. An explicit expression can be obtained as follows. Note that the scalar product can be expressed in terms of Gauss coefficients

$$\langle \Phi_1, \Phi_2 \rangle = R^2 \sum_{\ell,m} \frac{g_{1;\ell,m}\, g_{2;\ell,m}}{2\ell + 1} \tag{35}$$

where we considered Schmidt semi-normalization of spherical harmonics. Therefore defining Ξ in terms of the mapping of the Gauss coefficients, the operator will satisfy the above equations for:

$$\Xi : g_{\ell,m} \mapsto \frac{2\ell + 1}{R^2 \lambda_\ell^2} g_{\ell,m}. \tag{36}$$

In general this all we can say. However for the choices of λ_ℓ that we are considering below, more explicit expressions are possible.

In the following we show the corresponding operators Ξ for three choices of degree variances:

A- For potentials of *internal* origin Φ_I and choosing the degree variance $\lambda_\ell^2 = {}^1/(\ell+1)$, the corresponding operator can be identified through the following calculus:

$$\Gamma[\Phi_I] = \frac{1}{4\pi\, R^2} \int_{S_R} |\nabla \Phi_I(x)|^2\, \mathrm{d}\Omega_R(x) = \sum_{l,m} (\ell + 1) |g_{\ell,m}|^2. \tag{37}$$

We write this symbolically as $\Xi^{1/2} = \nabla$. By considering the correlation of potentials with *internal* origin – defined in Equation 23, we get

$$K_I(x, y) = R^2 \sum_\ell \frac{1}{(\ell + 1)}\, P_\ell(\hat{x} \cdot \hat{y}) \left(\frac{R^2}{|x||y|} \right)^{\ell+1} \tag{38}$$

which is directly associated with the generalized energy $\Gamma[\Phi_I]$ in Equation 37.

B- Choosing $\lambda_\ell^2 = {}^1\!/\!_l$ along with potentials of *external* origin, the operator is $\Xi^{1/2} = \nabla$ as well (in the sense that Eq 37 holds) and the energy is

$$\Gamma[\Phi_E] = \sum_{l,m} \ell \, |g_{\ell,m}|^2 = \Gamma[\mathbf{g}] \quad . \tag{39}$$

The associated correlation kernel is derived from Equation 27 and reads

$$K_E(x,y) = R^2 \sum_\ell \frac{1}{\ell} P_\ell(\hat{x}\cdot\hat{y}) \left(\frac{|x||y|}{R^2}\right)^\ell \quad , \tag{40}$$

again, this holds for *external* origin and degree variance $\lambda_\ell = {}^1\!/\!_\ell$.

C- The operator $\Xi = -(\mathbb{I} + 2r\partial_r)$ for internal fields, respectively $\Xi = (\mathbb{I} + 2r\partial_r)$ for external fields, is related with the degree variance $\lambda_\ell^2 = 1$ and the energy is

$$\Gamma[\Phi] = \sum_{l,m} |g_{\ell,m}|^2 = \Gamma[\mathbf{g}] \tag{41}$$

for both, internal and external origins. The associated correlation kernels for magnetic potentials follow from equations 23 and 27. They are

$$K_I(x,y) = R^2 \sum_\ell P_\ell(\hat{x}\cdot\hat{y}) \left(\frac{R^2}{|x||y|}\right)^{\ell+1} \tag{42}$$

$$K_E(x,y) = R^2 \sum_\ell P_\ell(\hat{x}\cdot\hat{y}) \left(\frac{|x||y|}{R^2}\right)^{\ell} \quad . \tag{43}$$

4 Some explicit kernels

In the following we are going to derive explicit kernel functions for the three correlation structures given in the previous section. In addition we consider the monopole and dipole case. These explicit formulas allow for an efficient numerical implementation of the kernels which avoids the computation of large sums of spherical harmonics. In fact by this technique we can effectively sum up all degrees without truncation.

4.1 Scalar kernels

Let us start with some introductory math. The degree variance we introduced in Equation 21 does not depend on the Gauss coefficient's order m. As a consequence, kernels $K(x,y)$ are rotational invariant – i.e. they depend only on rotational invariant quantities. These quantities are the scalar product $x^t y$ and the product magnitudes $|x||y|$. For both, potentials with internal or external origin, let us introduce a function $F(a,t)$ such that:

$$K_{(\cdot)}(x,y) = R^2\, F_{(\cdot)}(a,t) \qquad \text{with} \qquad a = \frac{|x||y|}{R^2} \qquad \text{and} \qquad t = \frac{x^t y}{R^2} \tag{44}$$

where the subscript $(\cdot)$ refers to an internal origin (I) or an external origin (E). For the kernels introduced in Equations 23 and 27 the functions F are

$$F_I(a,t) = \sum_{\ell=0}^{\infty} \lambda_\ell^2 \, a^{-(\ell+1)} P_\ell(t/a) \qquad |x| > R \tag{45}$$

$$F_E(a,t) = \sum_{\ell=0}^{\infty} \lambda_\ell^2 \, a^{\ell} P_\ell\left(t/a\right) = \tfrac{1}{a} F_I\left({}^1\!/\!{}_a, {}^t\!/\!{}_{a^2}\right) \qquad |x| < R \tag{46}$$

again, subscripts I and E refer to internal or an external origin, respectively.

For the so called monopole ($\lambda_\ell = \delta_{\ell,0}$) and the dipole ($\lambda_\ell = \delta_{\ell,1}$) it is trivial to derive kernel functions from Equations 45 and 46. We have for the internal and external monopole

$$F_I(a,t) = \frac{1}{a}, \quad F_E(a,t) = 1 \tag{47}$$

and for the internal and external dipole

$$F_I(a,t) = \frac{t}{a^3}, \quad F_I(a,t) = t. \tag{48}$$

Let us proceed with the analysis of Equations 45 and 46. Both can further be simplified by taking the Legendre Polynomial's generating function into account

$$\sum_{\ell=0}^{\infty} \rho^\ell P_\ell(\mu) = \frac{1}{\sqrt{1 - 2\rho\mu + \rho^2}} \tag{49}$$

with $-1 \leq \mu \leq 1$ and $0 < \rho < 1$.

Now, let $\lambda_\ell = 1$. Substituting $\rho = a$ and $\mu = \frac{t}{a}$ in Equation 49 we obtain

$$F_I(a,t) = F_E(a,t) = \frac{1}{\sqrt{1 - 2t + a^2}} =: L(a,t) \tag{50}$$

which is referred to as the Legendre kernel (LK). In geomagnetic application we might want to get rid of the monopole contained in LK. This can be achieved by subtracting the monopole terms from Equation 50, which results in

$$F_I(a,t) = L(a,t) - \frac{1}{a} \qquad \text{and} \qquad F_E(a,t) = L(a,t) - 1 \tag{51}$$

for internal and external origin, respectively.

Lets continue our analysis with a more complex degree variance $\lambda_\ell^2 = (\ell + 1)^{-1}$, $\lambda_0 = 0$. We again make use of the generating function employing a little trick. Integrating Equation 49 with respect to ρ results in

$$\int_0^\rho \frac{1}{\sqrt{1 - 2r\mu + r^2}} \, \mathrm{d}r = \sum_{\ell=0}^{\infty} \int_0^\rho r^\ell P_\ell(\mu) \, \mathrm{d}r = \sum_{\ell=0}^{\infty} \frac{1}{\ell+1} \rho^{\ell+1} P_\ell(\mu) \quad . \tag{52}$$

Substituting $\rho = {}^1\!/\!_a$ together with subtracting the monopole term yields

$$\sum_{\ell=1}^{\infty}(\ell+1)^{-1}a^{-(\ell+1)}P_\ell(\mu) = \int\limits_0^{1/a} \frac{1}{\sqrt{1-2r\mu+r^2}}\,\mathrm{d}r - \frac{1}{a} \tag{53}$$

and we realize that this is almost the kernel function for internal sources we are looking for. The integral in Equation 53 can be solved paying attention to the case $\mu = 1$ – i.e. $a = t$. By another substitution $\mu = {}^t\!/\!_a$ we obtain

$$F_I(a,t) = \begin{cases} -\log(a-t) + \log\left(1-t+\sqrt{1-2t+a^2}\right) - {}^1\!/\!_a & a \neq t \\ \log(a-1) - \log(a) - {}^1\!/\!_a & a = t \end{cases} \quad . \tag{54}$$

Now, we consider the case $\lambda_\ell^2 = \ell^{-1}$ without monopole term $\lambda_0 = 0$. Our calculus is similar to the previous case. First, we subtract the term for $\ell = 0$, than we factor out an a binging it to the other side. An integration by ρ and a substitution yields

$$\sum_{\ell=1}^{\infty}\ell^{-1}a^\ell P_\ell(\mu) = \sum_{\ell=1}^{\infty}\int_0^a \frac{1}{r}\,r^\ell P_\ell(\mu)dr \int_0^a \frac{1}{r}\left(\frac{1}{\sqrt{1-2r\mu+r^2}} - 1\right)\mathrm{d}r \tag{55}$$

which is the kernel function for external sources. By solving the integral we get

$$F_E(a,t) = -\log\left(1-t+\sqrt{1-2t+a^2}\right) \quad . \tag{56}$$

The presented analysis establishes a series of analytic expressions for correlation functions of internal and external origins which correspond to kernels introduced in Equations 38, 40, 42 and 43.

4.2 Vector fields

Magnetic vector field observations, make the calculation of the kernel's gradient necessary. As we will show in Equations 63 and 64, the correlation matrix consists of the gradient with respect to locations x and y of the kernel $K(x,y) = R^2F(t,a)$. To calculate gradients it is convenient to introduce the following quantities:

$$\begin{aligned} \nabla a &= \frac{\hat{x}|y|}{R^2}\,, & a\nabla^t &= \frac{|x|\hat{y}^t}{R^2}\,, & \nabla a\nabla^t &= \frac{\hat{x}\hat{y}^t}{R^2}\,, \\ \nabla t &= \frac{y}{R^2}\,, & t\nabla^t &= \frac{x^t}{R^2}\,, & \nabla t\nabla^t &= \frac{\mathbb{I}}{R^2}\,. \end{aligned} \tag{57}$$

Then, the kernel's gradient can be expressed through partial derivatives $F_a = \partial_a F$, $F_{aa} = \partial_a^2 F$, $F_t = \partial_t F$, $F_{tt} = \partial_t^2 F$, $F_{ta} = \partial_t\partial_a F$ where F refers either to F_I or F_E. Having all these quantities defined, gradients can be expressed as follows:

$$\nabla K(x,y) = R^2\left(\nabla a\ F_a + \nabla t\ F_t\right) = \hat{x}|y|\ F_a + y\ F_t \tag{58}$$

and

$$\nabla K(x,y)\nabla^t = \hat{x}\hat{y}^t(F_a + aF_{aa}) + \hat{y}\hat{x}^t aF_{tt} + (\hat{x}\hat{x}^t + \hat{y}\hat{y}^t)aF_{ta} + \mathbb{I}F_t. \tag{59}$$

and Legendre Kernel.

Numerical calculation requires some caution because of F's singularities that may occur when $t = a$. However, these singularities are well resolved when taking the derivatives – e.g. see Shure et al. (1982).

5 How to work with these kernels

The following section describes the entire workflow to invert for a model of the magnetic field from magnetic vector field observations $\tilde{\mathbf{B}}$. To keep that section concise we assume the magnetic field consists of three parts only:

$$\Phi = \Phi_I + \Phi_E + \epsilon \tag{60}$$

One field/potential of internal origin (I), one field of external origin (E) and observational noise. For simplicity measurement noise is assumed to be *i.i.d.* Gaussian distributed with known variance. In Section 6, our case study, we present an extension to a higher number of source regions.

We start with a model that is defined by the magnetic field at locations of observation. In the next subsections we also consider a model based on the magnetic field on a series of points on the sphere. Finally a model predicting Gauss coefficients will be presented.

In Appendix A, we show in which sense the solutions we obtain are equal to those, one obtains using harmonic splines with norm minimising regularisation.

5.1 modelling magnetic field components at observation points

If we neglect coupling effects between the internal and external fields, we assume each component to be modelled by distinct correlation kernels. Then the correlation of the total field is simply the sum of both kernels. By introducing adjustable scaling factors α_I and α_E we the field's total kernel reads

$$K = \alpha_I^2 K_I + \alpha_E^2 K_E \quad . \tag{61}$$

In their abstract forms, the correlation kernels K_I and K_E are given by Equations 23 and 27, however, to use them, some parameters need to be determined first:

- The reference radii R_I and R_E.
- Scaling amplitudes α_I and α_E.
- The degree variances λ_ℓ^2.

In principle, the degree variances can be specified a priori. As already outlined in Section 3.3, common choices in magnetic field modelling are $\lambda_\ell^2 = (l+1)^{-1}$ for internal sources (Eq. 38) (Shure et al., 1982), and $\lambda_\ell^2 = l^{-1}$ for external sources (Eq. 40). For $\lambda_\ell = 1$ the kernels are easier to implement numerically. These degree variances lead to closed form expressions which, in addition, produce acceptable a priori models of the potential. Reference radii and scaling factors can be retrieved from observations. In order to do so we propose a maximum likelihood estimate (see Section 6.1).

As already mentioned, we consider a dataset of magnetic vector field observations $\tilde{\mathbf{B}} = [\mathbf{B}(x_k)]_{k=1,\dots,N}$ at N sampling points x_k (e.g. the observatory sites). Which means to measure a $3N$ values i.e. three components at each location. Those components are determined by three directions $\mathbf{e}_n$ e.g. *north*, *east* and *down* components. Once we got a reasonable estimate of the Kernels' parameters we proceed in building the correlation matrices. The kernel function for fields of internal origin is defined by

$$\mathbb{E}[\Phi_I(x)\,\Phi_I(y)] = \alpha_I^2 K_I(x, y) \quad . \tag{62}$$

Then the elements of the correlation matrix $\mathbf{C}^I$ for magnetic vector field observations is given by

$$C^I_{k,k'} = \alpha_I^2 \left(\mathbf{e}_k^t \cdot \nabla K_I(x_k, x_{k'}) \nabla^t \cdot \mathbf{e}_{k'} \right) \tag{63}$$

where $\mathbf{e}_k$ and $\mathbf{e}_{k'}$ are the vector directions of observations at the N sampling points x_k and $x_{k'}$, respectively. In the same manner we derive the correlation matrix for the component of external origin:

$$\mathbf{C}^E = \alpha_E^2 \left[\mathbf{e}_k^t \cdot \nabla K_E(x_k, x_{k'}) \nabla^t \cdot \mathbf{e}_{k'} \right]_{\{k,k'\}} \tag{64}$$

Again, because we do not consider coupling amongst components – e.g. induction effects – the total covariance matrix for our set of observations is

$$\Sigma_{\mathbf{BB}} = \mathbf{C}^I + \mathbf{C}^E + \mathbf{C}^\epsilon \quad , \tag{65}$$

where $\mathbf{C}^I$ and $\mathbf{C}^E$ are the observational correlation matrices for fields of internal and external origin and $\mathbf{C}^\epsilon$ the covariance matrix related to measurement noise. Typically, noise is assumed to be uncorrelated, thus, the matrix $\mathbf{C}^\epsilon$ is diagonal. Therefore, $\Sigma_{\mathbf{BB}}$ is not singular and can be inverted without major difficulties.

Once we have the data's correlation matrix, we proceed with the approach outlined in Section 2 and compute the conditional distribution (Eq. 12) knowing $\tilde{\mathbf{B}}$. At points of observations the total field is decomposed into its components by

$$\begin{aligned} \overline{\mathbf{B}}^I_{|\tilde{\mathbf{B}}} &= \mathbf{C}^I\,\Sigma^{-1}_{\mathbf{BB}}\,\tilde{\mathbf{B}} \\ \overline{\mathbf{B}}^E_{|\tilde{\mathbf{B}}} &= \mathbf{C}^E\,\Sigma^{-1}_{\mathbf{BB}}\,\tilde{\mathbf{B}} \\ \overline{\mathbf{B}}^\epsilon_{|\tilde{\mathbf{B}}} &= \mathbf{C}^\epsilon\,\Sigma^{-1}_{\mathbf{BB}}\,\tilde{\mathbf{B}} \, . \end{aligned} \tag{66}$$

Clearly the components sum up to the total observed field by the definition of $\Sigma_{\mathbf{BB}}$. The posterior covariances which quantify the uncertainties of these components are given by

$$\begin{aligned}
\mathbf{C}^I_{|\tilde{\mathbf{B}}} &= \mathbf{C}^I - \mathbf{C}^I \, \Sigma^{-1}_{\mathbf{BB}} \, \mathbf{C}^I \\
\mathbf{C}^E_{|\tilde{\mathbf{B}}} &= \mathbf{C}^E - \mathbf{C}^E \, \Sigma^{-1}_{\mathbf{BB}} \, \mathbf{C}^E \\
\mathbf{C}^\epsilon_{|\tilde{\mathbf{B}}} &= \mathbf{C}^\epsilon - \mathbf{C}^\epsilon \, \Sigma^{-1}_{\mathbf{BB}} \, \mathbf{C}^\epsilon \, .
\end{aligned} \tag{67}$$

The above, presents a method to separate field components, however, at points of observation only. The following Section shows how to predict the magnetic field at a set of so called *design points* which do not coincide with the points of observations.

5.2 Estimating field components outside of observation points

Now we want to estimate the magnetic field components at locations for which there are no observations. Therefore we define a set of design points $\{y_m\}$, $m = 1, \ldots, M$, e.g. a regular grid. At those design points, the three component vector of the magnetic field are defined by three directions $\mathbf{e}_m$ e.g. unit vectors of a Cartesian reference frame. The predicted $3M$ components of the magnetic field at the M observation points y_m are collected in a vector $\mathbf{m}$. As before, we adopt notations introduced in Section 2 (Eqs. 10 and 11). The correlation matrix, linking the observations with predictions at the design points, is

$$\Sigma_{\mathbf{mB}} = \alpha^2_{(\cdot)} \left[\mathbf{e}^t_m \cdot \nabla K_{(\cdot)}(y_m, x_k) \nabla^t \cdot \mathbf{e}_k \right]_{\{m,k\}} \tag{68}$$

where index $k = 1, \ldots, N$ and direction $\mathbf{e}_k$ refer to the observations $\mathbf{B}(x_k)$ and the free subscript denotes for internal or external origin.

If we again assume the a priori potential to be of zero mean – i.e. $\overline{\Phi} = 0$ – then $\overline{\mathbf{m}} = 0$ and $\overline{\mathbf{B}} = 0$. Following Equation 12, the posterior expectation at points were we want to predict is

$$\overline{\mathbf{m}}_{|\tilde{\mathbf{B}}} = \Sigma_{\mathbf{mB}} \, \Sigma^{-1}_{\mathbf{BB}} \, \tilde{\mathbf{B}} \, . \tag{69}$$

The field-component's prior correlation matrix is given by

$$\Sigma_{\mathbf{mm}} = \left[\mathbf{e}^t_m \cdot \nabla K_{(\cdot)}(y_m, y_{m'}) \nabla^t \cdot \mathbf{e}_{m'} \right]_{\{m,m'\}} \, , \tag{70}$$

where y_m and $\mathbf{e}_m$ refer to our design points together with directions and $m, m' = 1, \ldots, 3M$. Following once more Equation 12 leads to the posterior correlation matrix

$$\Sigma_{\mathbf{mm}|\tilde{\mathbf{B}}} = \Sigma_{\mathbf{mm}} - \Sigma_{\mathbf{mB}} \Sigma^{-1}_{\mathbf{BB}} \Sigma^t_{\mathbf{mB}} \, . \tag{71}$$

Note that this relation holds for given radii and scaling factors. Taking uncertainties in those quantities into account renders the posterior non-Gaussian. This, however, will be subject to a forthcoming publication.

5.3 Estimating other linear observables

It is possible to generalize the above approach for linear functionals, where linearity is considered with respect to the magnetic potential Φ. In the following, we illustrate this by giving two examples. First, we show how to estimate the potential it self. Second, we predict the potential's Gauss coefficients.

For estimating the components of the magnetic potential we consider the same M design points $\{y_m\}$, introduced in the previous section. $m = 1, \ldots, M$. Let us call $\mathbf{p}$, a model that consists of magnetic potential values at the modelling points. Then, to find a solution for such a model, the equations 69 and 71 should be used replacing $\Sigma_{\mathbf{mB}}$ by:

$$\Sigma_{\mathbf{pB}} = \alpha_I^2 \, [K_I(y_m, x_k) \nabla_{x_k}^t \cdot \mathbf{e}_k]_{\{m,k\}} \ , \tag{72}$$

and $\Sigma_{\mathbf{mm}}$ by:

$$\Sigma_{\mathbf{pp}} = \ [K_I(y_m, y_{m'})]_{\{m,m'\}} \ . \tag{73}$$

Because we keep observations untouched, the matrix $\Sigma_{\mathbf{BB}}$ remains as in Equation 65.

The relation between the Gauss coefficients and the magnetic potential is given by equation 19. To find the correlation between the Gauss coefficients and the magnetic field measurements, one has to use the relation 72, expend the expression of the kernel given in equation 23, and integrate over the sphere of radius R. If we call $\mathbf{g}$ the model vector made of Gauss coefficients of degree and order $\{l, m\}$, it is obtained:

$$\Sigma_{\mathbf{gB}} = \alpha_I^2 \, [R \, \{\lambda_\ell^2 \, Y_{\ell,m}(\hat{x}_k) \left(\frac{R}{|x|}\right)^{\ell+1} \} \nabla_{x_k}^t \cdot \mathbf{e}_k]_{\{l,m,k\}} \ , \tag{74}$$

where the reference radius of the Gauss coefficients is R. By construction, it is obvious that the correlation matrix of the model is:

$$\Sigma_{\mathbf{gg}} = \ [\lambda_\ell^2 \ \delta_{\ell,\ell'} \delta_{m,m'}]_{\{\ell,m,\ell',m'\}} \ . \tag{75}$$

The solution is as before defined by the posterior expected values and the covariances of the Gauss coefficients. These are obtained from equations 69 and 71, replacing $\Sigma_{\mathbf{mB}}$ and $\Sigma_{\mathbf{mm}}$ by $\Sigma_{\mathbf{gB}}$ and $\Sigma_{\mathbf{gg}}$ respectively.

6 A case study for field inversion

To illustrate how this technique can be used to separate various field components, hourly mean observatory data, as provided by Macmillan and Olsen (2013) are used. We estimated the average of these means over January 2001. By taking an average over a month the contribution of the induced fields is significantly reduced. Any observatory presenting a crustal offset larger than 1500nT in intensity, as estimated with the GRIMM model (Lesur et al., 2015), is discarded. This leads to a total of $N = 105$ observatory, providing each three component vector measurements.

As already introduced in Section 2, we consider in our modelling approach four magnetic field components with observational noise atop. Those components are the core field, the lithospheric field, the ionospheric and magnetospheric contributions. In addition, due its dominance, the core field's dipole component is treated separately. Again, we are neglecting any coupling effects – i.e. we a priori assume components to be independent from one another. Accordingly, the total covariance structure is of the following form:

$$K = \alpha_C^2 K_C + {\alpha_C^D}^2 K_C^D + \alpha_L^2 K_L + \alpha_I^2 K_I + \alpha_M^2 K_M + \sigma^2 K_N \tag{76}$$

(compared with equation 5 a noise and dipole component had been set in). The measurement noise is assumed to be known and set to $\sigma^2 = (4\,\mathrm{nT})^2$. Thus, coefficients α_C, α_C^D, α_L, α_I and α_M are necessary to adjust for the contribution of the core, lithospheric, ionospheric and magnetospheric fields. For the correlation structures we consider the Legendre Kernel (LK) without monopole contributions. We prefer, LK due to simpler equations and slightly better conditioned correlation matrices. Since our kernels $K_{(\cdot)}$ have a dependence on the radius $R_{(\cdot)}$, each component has an additional parameter. These are R_C (for the core field and its dipole), R_L, R_I, and R_M, associated with their corresponding correlation structures. Note that these are not necessarily the true position of the sources, but rather an effective radius which explains best the observed correlations.

6.1 Parameter estimation

To estimate the 9 parameters defining the correlation structures – the four radii and five factors – we use a maximum likelihood approach. The a priori covariance structure of the field observations $\tilde{\mathbf{B}}(x_m)$ is obtained by evaluating the gradients of the kernels at the points of observations x_m, $m = 1, \ldots, M$. Supposing we have measured all 3 components at each of the points x_m, we have $N = 3N$ measurements B_k at position x_k, $k = 1, \ldots, K = 3M$. Note that the same position appears thre times in this list. Then the correlation matrix reads

$$\mathbf{C}_{k,k'}^{(\cdot)} = \alpha_{(\cdot)}^2 \left\{ \mathbf{e}_k^t \cdot \nabla K_{(\cdot)}(x_k, x_{k'}) \nabla^t \cdot \mathbf{e}_{k'} \right\} \qquad \text{with} \qquad k = 1, \ldots, N \tag{77}$$

where $(\cdot)$ refers to core, core dipole, lithosphere, ionosphere and magnetosphere, respectively. The total correlation structure reads

$$\mathbf{C} = \mathbf{C}^C + \mathbf{C}^{C,D} + \mathbf{C}^L + \mathbf{C}^I + \mathbf{C}^M + \sigma^2 \mathbb{I} \tag{78}$$

where $\mathbb{I}$ denotes the $3N \times 3N$ identity matrix. For our Gaussian model, the likelihood function reads

$$L\Big(\theta = (R_C, R_L, R_I, R_M, \alpha_C, \alpha_C^D, \alpha_L, \alpha_I, \alpha_M) \Big| \{\tilde{\mathbf{B}}(x_k)\}_{k=1,\ldots,N}\Big) \propto \\ \propto \frac{1}{\sqrt{\det \mathbf{C}}} \exp\Big\{ -\tfrac{1}{2} \tilde{\mathbf{B}}^t \mathbf{C}^{-1} \tilde{\mathbf{B}} \Big\} \tag{79}$$

Core	$R_C = 2658.2\,\text{km}$	$\alpha_C = 84478.0$	$\alpha_C^D = 226351.0$
Lithosphere	$R_L = 6340.6\,\text{km}$	$\alpha_L = 0.1318$	
Ionosphere	$R_I = 6377.6\,\text{km}$	$\alpha_I = 0.00019$	
Magnetosphere	$R_M = 24002.5\,\text{km}$	$\alpha_M = 0.00013$	
Noise		$\sigma^2 = 16.0$	

Table 1: Parameters we find by maximizing the likelihood function (Eq. 79).

In order to estimate the parameters, we maximize the likelihood function

$$\hat{\theta}_{\text{mle}} = \arg\max_{\theta} L\Big(\theta \,\Big|\, \{\tilde{\mathbf{B}}(x_k)\}_{k=1,\ldots,N}\Big) \tag{80}$$

where θ denotes for the nine parameters to adjust. Instead of trying to derive a closed-form solution to the maximization problem, we are using numerical optimization methods to find the Maximum Likelihood Estimator (MLE). The values we obtained are given in Table 1.

6.2 Field inversion

The radii and magnitudes found previously and given in Table 1 are now used as prior information for the evaluation of the core, lithospheric, iononspheric and magnetospheric field models. A first inversion is performed at the observatories locations (shown with red triangles in figure 2) as detailed in section 5.1. The mean fields and posterior covariances are then considered to build a spherical harmonics model as presented in section 5.3. However the posterior variances of the lithospheric, iononspheric and magnetospheric field are so large that no useful information can be extracted on them. Therefore, we focus on the mean core field that we refer as B_C. The latter is expanded in spherical harmonic up to degree 30 and its coefficients are evaluated at the level of the Earth's surface. The results we obtained are compared to the core field model GRIMM 3 of Mandea et al. (2012) for the epoch 2001.0 and referred as B_G.

In figure 1 the energy spectrum of B_C and B_G are respectively plotted with a black line and with circles. The behaviour of both spectra is similar up to spherical harmonic degree $l = 7$. From there, the spectrum of B_C decreases at a much faster rate than the spectrum of B_G. When looking at the posterior variance (dashes), one can clearly observe that from degree $l = 8$, it becomes more intense than the energy contained in the scales of the mean core field itself. At high degree, the posterior variance tends towards the prior variance (dotted line), indicating that the data do not carry information on the core field at these degree.

The posterior variance provides an estimate of the uncertainties associated with the mean field. Since magnetic field model derived from satellite data, such as the GRIMM 3 model, are much more precise than our model derived from observatory data, we can consider that it is a good approximation of the real magnetic field. Therefore the difference between B_C and B_G should be of

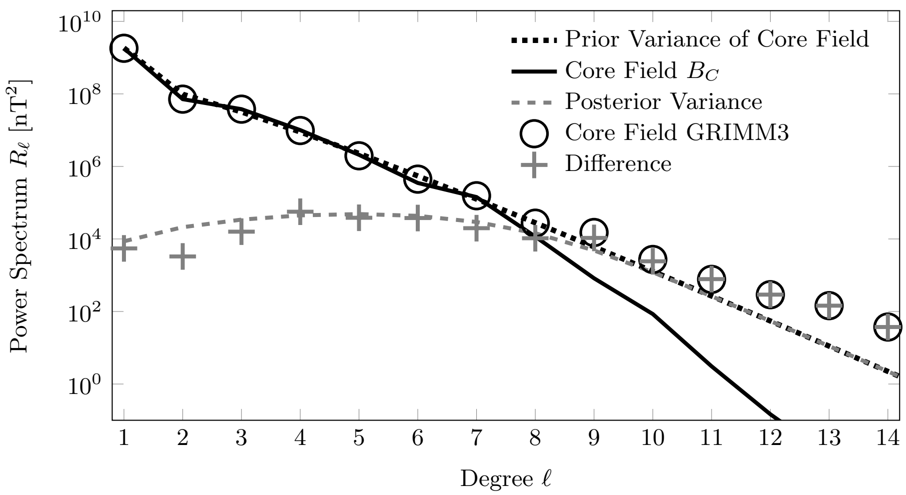

Figure 1: Energy spectra at the Earth's surface of B_C (black line) and GRIMM3 core field (circles). Prior variances (dotted line) and posterior variances (dashes). Spectrum of the difference between the core field of GRIMM3 and B_C (crosses).

the order of the predicted uncertainties. Yet, the energy spectrum associated with the error field $B_C - B_G$, is slightly spreading around the posterior variance, showing that the posterior statistics we obtain are realistic.

Having access to the full posterior distribution of the core magnetic field, it is possible to study locations where the field model is more or less accurate. In figure 2, iso-contour of the declination and inclination are respectively displayed on the top left and on the bottom left, together with their 90% confidence intervals in degree (color maps). A strong correlation between high observatory density and accuracy of the declination and inclination can be observed. Indeed, in the northern hemisphere, which is well covered by observatories, declination and inclination present a low posterior variability. On the contrary, in areas of poor coverage, such as in the Pacific ocean or in the southern part of the Atlantic, uncertainties become large. When looking at the difference in absolute value between the declination and inclination associated with B_C and the ones associated with B_G (top right and bottom right of figure 2 respectively), one can see that areas of weak posterior variability correspond to areas where the difference is weak, whereas locations where the difference is large, always correspond to locations where the predicted variability was large.

7 Discussion and conclusion

We have shown how to define and use kernel based correlation structures to model internal and external magnetic field components.

We originally started this work with the objective of approaching the geo-

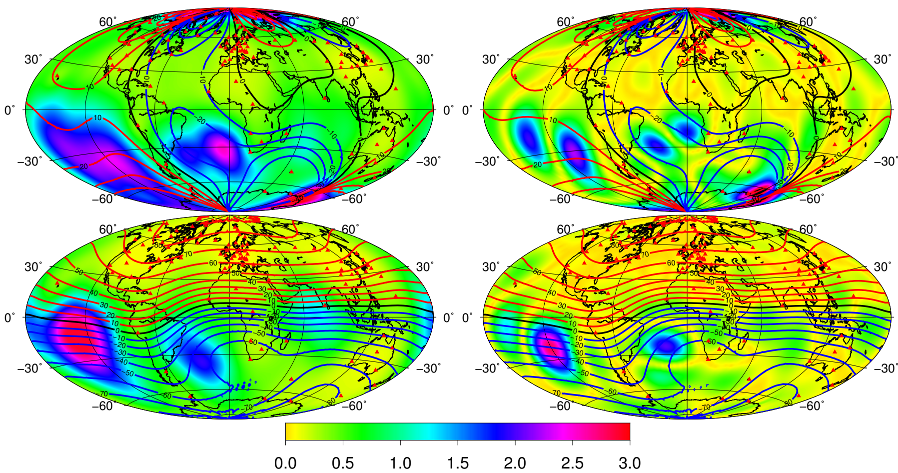

Figure 2: Iso lines: declination (top) and inclination (bottom) associated with the B_C field (left) and the GRIMM3 core field (right). Color maps: 90% confidence on the declination (top left) and inclination (bottom left) in degree, and difference between the GRIMM3 and B_C's declinations (top right) and inclinations (bottom right) in degree. The red triangles indicate the locations of observatories used in the inversion.

magnetic field modelling using a technique where all constraints applied on the model are explicit. This is in contrast to the usual spherical harmonic representation method where models are arbitrarily truncated to low degrees, and time dependences strongly reduced or smoothed. The approach we proposed uses correlation structures. In principle these could be derived from the physics of the sources contributing to the magnetic field – e.g. correlation structures can be derived from numerical dynamo codes for the contribution of the core field (Aubert, 2014). If the source is not known well enough, we propose and use correlation structures that, each, require only two parameters: a radius where the Gauss coefficients are uncorrelated and a scaling factor. We have shown that these correlation structures have the same form as harmonic splines (Shure et al., 1982), and that the approach we propose is strictly equivalent to the usual constrained least-squares approach used with these types of basis functions. We nonetheless extend this technique for all type of sources either from internal and external origins.

As explained, the correlation structures we defined rely on three points:

- the assumption that it exist a spherical surface where the Gauss coefficients are uncorrelated for all SH degrees,
- the radius of this surface,
- and a scaling factor for the obtained correlation structure.

These radius and the scaling act as tuning parameters that define the spatial correlation length of the signal at observation points and its energy. Whatever value is given to the former parameter – i.e. the radius, the correlation structure of a given source can be used to model the full data set, independently of the types of signals that contribute to these data. However, modelling a signal from external origin using e.g. the correlation structure of the core field, requires the core field to have unrealistic energy. The energy associated with a source is controlled through the scaling factor. So, given a data set with a characteristic distance between sampling points, the signals of all sources that have long enough correlation length can be separated between them and from the noise, if their scaling factor is properly set. We have therefore a new technique to efficiently separate contributions from internal and external origins in observatory and satellite data.

We applied the technique to a set of three component magnetic field monthly averages made from observatory hourly mean data. This data set was analysed assuming four sources; the core, lithosphere, ionosphere and magnetosphere. We neglected the induced field to avoid having to deal with contributions from internal and external origin correlated in space and time. To separate the four contributions, we were planning to impose the radii and scaling factors by hand, but it turns out that these can be estimated from the magnetic data themselves. The separation of the core field and magnetospheric field is likely due to the fact that the largest wavelengths of an external field (SH degree 1 and 2) cannot be easily described by an internal field (Lesur et al., 2008). These two first SH degrees define therefore the magnetospheric correlation structure radius and scaling. The core field radius and scaling are robustly imposed by the internal field signals from SH degree 1 to 7. The separation with the lithospheric field is only possible due to a detectable internal signal at higher SH degree that is not compatible with the correlation structure of the core field. This signals can be detected only by observatories in Europe and Northern America where the observatory density is high enough to reveal relatively short wavelengths. The separation of the lithosphere and ionosphere contributions and the noise is not possible with the data set in hand, so the noise level has to be imposed by hand, and we find equivalent energies for the ionosphere and lithosphere. These two later contributions are not well separated. We have not accounted for the local lithospheric field component at the observatory locations – i.e. the crustal offsets, and we have noticed a related noise at SH degree 7 to 9 in the core field model. A field model of higher quality would be obtained if these offsets are estimated independently and subtracted.

The technique we proposed and describe in this paper allow potentially significant progress in magnetic field modelling. It first permit a separation of contributions from field of internal and external origins in a consistent and well controlled way. Particularly, the spherical harmonic expansion for each model component is infinite, and not, as in classic models, truncated to the few first SH degree for the magnetospheric component. These infinite expansions can nonetheless be computed explicitly and are numerically easy to implement. The main limitation of the method is that the number of parameter of the model is, as for collocation methods in gravity, as large as the number of sampling points. The method is therefore particularly well suited for observatory data analysis, but its application to satellite data remains a challenge.

We have mainly shown here examples and applications that involved linear relationship between correlation structures and observable. The method can also, in principle, be applied to none-linear data as the magnetic inclination, declination and total intensity. This is a prerequisite to apply this modelling technique to historical records and paleomagnetic data.

Finally we point out that by using a Bayesian approach to model the magnetic field, we do not define a specific set of parameters for a model, as it is done with a classic least squares approach. Rather, we define a Gaussian distribution of models, fully described by its mean and variance. A model, made of the combination of correlation structures for the different sources is valid, if the posterior distributions of each of the model component are in agreement with their prior distributions. If a model is valid, then we have realistic information on the variance of the output mean model. This is an information that is not provided by any of the other modelling approach proposed so far.

Acknowledgements

This work would not have been possible without the provision of observatory data, and therefore the work of the scientists and technicians in observatories. Vincent Lesur has started this work while invited professor at ETH Zürich. He was formerly at the German Research Center for Geosciences (GFZ), Postdam. Julian Baerenzung is supported by the priority program *Planetary Magnetism* (SPP1488) of the German Research Foundation (DFG). Furthermore, the support of Stefan Mauerberger by the Helmholtz Graduate Research School GeoSim is acknowledged. This is the IPGP contribution XXXXXXXX . . .

A Link between correlation and spline modelling techniques

Classical spline modelling finds a model that is a compromise between smoothness and fit to the data. This is the approach used for most of the magnetic field models established in the recent years. The relation between spline modelling and our correlation approach can be summarised by saying that the spline solution is simply the posterior expected value of the model that is derived through the correlation approach, given the observations. In the following we present this statement in greater details. We present first the case of perfect data and then the case of uncertain data.

First note the following particularity of the scalar product associated with the energy Γ in equation 34. The scalar product of two kernels at distinct positions x and y is

$$\Gamma[K(\cdot, x), K(\cdot, y)] = K(x, y) \tag{81}$$

which is the reproducing kernel equation. Any function $\Phi(x)$ that can be written as the superposition of kernels $\Phi(x) = \sum \alpha_k K(x, x_k)$, therefore, satisfies the equation

$$\Phi(x) = \Gamma[K(x,y), \Phi(y)] \ . \tag{82}$$

Integration here is understood with respect to y. Actually, all functions that have finite generalised energy can be approximated arbitrarily well by such a superposition of kernels. The closure of these sums forms the Hilbert space associated with the reproducing kernel K.

Let assume that are given K, noise free measurements $\tilde{B}_k$, $k = 1, \ldots, K$ of the magnetic field $\mathbf{B}$ at points x_k, in direction $\mathbf{e}_k$:

$$\tilde{B}_k = -\mathbf{e}_k^t \cdot \nabla\Phi(x_k) \ . \tag{83}$$

The interpolatory spline solution is then the magnetic potential Φ that minimizes the energy $\Gamma[\Phi]$ given in equation 34, under the observational constraints. Introducing the constraints in equation 82 gives:

$$\mathbf{e}_k^t \cdot \nabla\Phi(x_k) = \Gamma[\mathbf{e}_k^t \cdot \nabla K(x_k, x), \Phi(x)] = \Gamma[\Phi(x), K(x, x_k)\nabla^t \cdot \mathbf{e}_k], \tag{84}$$

and the optimization problem is reduced to the problem of minimising $\Gamma[\Phi] = \Gamma[\Phi, \Phi]$ under the constraints:

$$\Gamma[\Phi(x), K(x, x_k)\nabla^t \cdot \mathbf{e}_k] = -\tilde{B}(x_k). \tag{85}$$

As for any scalar product, the solution $\hat{\Phi}$ to this constrained optimisation problem is a linear combination of kernels:

$$\hat{\Phi}(x) = \sum_k \alpha_k K(x, x_k)\nabla^t \cdot \mathbf{e}_k, \tag{86}$$

and the observational constraints are:

$$\begin{aligned} \tilde{B}_k = & \quad -\mathbf{e}_k^t \cdot \nabla\hat{\Phi}(x_k) \quad \text{for } k = 1, \cdots, K, \\ = & \quad -\textstyle\sum_{k'} C_{k,k'}\, \alpha_{k'} \end{aligned} \tag{87}$$

with the elements of the matrix $\mathbf{C}$ being:

$$C_{k,k'} = \mathbf{e}_k^t \cdot \nabla K(x_k, x_{k'})\nabla^t \cdot \mathbf{e}_{k'} \ . \tag{88}$$

We note that $\mathbf{C}$ is the a priori correlation matrix between the field components at the observation points (see e.g. equation 63). As long as the observations are all different, it can be inverted and:

$$[\alpha_k]_{\{k\}} = \mathbf{C}^{-1} \cdot [\tilde{B}_k]_{\{k\}}. \tag{89}$$

Therefore, the expression 86 giving the solution of the optimisation problem is also the posterior expectation for the magnetic potential, given the observations:

$$\hat{\Phi}(x) = \mathbb{E}(\Phi(x)|\{\tilde{B}_k\}_k) \ . \tag{90}$$

The magnetic field is obtained by:

$$\begin{aligned}\hat{\mathbf{B}}(x) = & \quad -\mathbf{e}_k^t \cdot \nabla\hat{\Phi}(x) \\ = & \quad \mathbb{E}(\mathbf{B}(x)|\{\tilde{B}_k\}_k) \ ,\end{aligned} \tag{91}$$

and at the observation points and directions,

$$[\hat{B}_k]_{\{k\}} = \mathbf{C} \cdot [\alpha_k]_{\{k\}}. \tag{92}$$

Finally, the expression for the generalized energy as a function of the α_k is:

$$\Gamma[\Phi, \Phi] = [\alpha_k]_{\{k\}}^t \cdot \mathbf{C} \cdot [\alpha_k]_{\{k\}}. \tag{93}$$

Now we consider the case of noisy observations:

$$\tilde{B}_k = -\mathbf{e}_k^t \cdot \nabla\Phi(x_k) + \epsilon_k, \tag{94}$$

where the measurement errors are normally distributed with zero mean and with a correlation:

$$\mathbb{E}(\epsilon_k, \epsilon_{k'}) = \sigma_{k,k'}^2. \tag{95}$$

We seek the noise free values of the magnetic field at the observation points and directions: $[B_k]_{\{k\}}$. As before, the correlation matrix between the observations is:

$$\mathbf{\Sigma_{BB}} = \mathbf{C} + \mathbf{C}^\epsilon, \tag{96}$$

where we assume that the measurement errors are not correlated to the magnetic field and that $\mathbf{C}^\epsilon$ is the covariance matrix of the noise defined in equation 95. Because we want to obtain noise free values of the magnetic field components at observation points, the correlation between model and observation is $\mathbf{\Sigma_{mB}} = \mathbf{C}$ and thus the expected value for the model is:

$$\mathbb{E}([B_k]_{\{k\}}|\{\tilde{B}_k\}_k) = \mathbf{C} \cdot (\mathbf{C} + \mathbf{C}^\epsilon)^{-1} \cdot [\tilde{B}_k]_{\{k\}}, \tag{97}$$

if we assume that the vectors $[B_k]_{\{k\}}$ and $[\tilde{B}_k]_{\{k\}}$ have zero prior expected value. On the other hand the spline solution consists in minimizing a compromise between fit to the data and generalized energy

$$E = \Gamma[\Phi, \Phi] + \sum_{k',k} \frac{(-\mathbf{e}_{k'} \cdot \nabla\Phi(x_{k'}) - \tilde{B}_{k'})(-\mathbf{e}_k \cdot \nabla\Phi(x_k) - \tilde{B}_k)}{\sigma_{k',k}} \tag{98}$$

Using equations 92 and 93, this energy can be expressed in matrix form:

$$\begin{aligned}E = & \quad [\alpha_k]_{\{k\}}^t \cdot \mathbf{C} \cdot [\alpha_k]_{\{k\}} \\ & + \left([\tilde{B}_k]_{\{k\}} - \mathbf{C} \cdot [\alpha_k]_{\{k\}}\right)^t \cdot \mathbf{C}^{-\epsilon} \cdot \left([\tilde{B}_k]_{\{k\}} - \mathbf{C} \cdot [\alpha_k]_{\{k\}}\right) \ ,\end{aligned} \tag{99}$$

where $\mathbf{C}^{-\epsilon}$ is the inverse of the matrix $\mathbf{C}^\epsilon$. Minimizing this energy for the α_k leads to the usual solution:

$$[\hat{\alpha}_k]_{\{k\}} = \left(\mathbf{C}^t \cdot \mathbf{C}^{-\epsilon} \cdot \mathbf{C}\right)^{-1} \mathbf{C}^t \cdot \mathbf{C}^{-\epsilon} \cdot [\tilde{B}_k]_{\{k\}} \ , \tag{100}$$

and, through equation 92, to the solution – i.e. the noise free magnetic field components at the sampling points:

$$[\hat{B}_k]_{\{k\}} = \mathbf{C} \cdot \left(\mathbf{C}^t \cdot \mathbf{C}^{-\epsilon} \cdot \mathbf{C}\right)^{-1} \mathbf{C}^t \cdot \mathbf{C}^{-\epsilon} \cdot [\tilde{B}_k]_{\{k\}} \ . \tag{101}$$

Using the Woodburry matrix identity, it is obtained that this solution is the same as equation 97. This shows again that the spline solution $\hat{\mathbf{B}}(x)$ is again the posterior mean of the distribution solution of our correlation based method:

$$\hat{\mathbf{B}}(x_{k'}) = \mathbb{E}(\mathbf{B}(x_{k'})|\{\tilde{B}_k\}_k) \ . \tag{102}$$

Generalisation to more complex models is cumbersome but straightforward. The key point here is that the solution of the optimisation problem can be computed as a superposition of kernels, as in equation 86.

References

Lesur, V., Whaler, K., and Wardinski, I. (2015), Are geomagnetic data consistent with stably stratified flow at the core-mantle boundary?, *Geophys. J. Int.*, 201(2):929 – 946, doi:10.1093/gji/ggv031

Sabaka, T. J., Olsen, N., Tyler, R. H., and Kuvshinov, A. (2015), CM5, a pre-swarm comprehensive geomagnetic field model derived from over 12 yr of CHAMP, Ørsted, SAC-C and observatory data, *Geophys. J. Int.*, 200(3):1596–1626, doi:10.1093/gji/ggu493

Aubert, J. (2014), Earth's core internal dynamics 1840-2010 imaged by inverse geodynamo modelling, *Geophys. J. Int.*, 197:1321–1334, doi: 10.1093/gji/ggu064

Chulliat, A. and Maus, S. (2014), Geomagnetic secular acceleration, jerks, and localized standing wave at the core surface from 2000 to 2010, *Journal of Geophysical Research (Solid Earth)*, doi:10.1002/2013JB010604

Olsen, N., Lühr, H., Finlay, C., Sabaka, T. J., Michaelis, I., Rauberg, J., and Tøffner-Clausen, L. (2014), The chaos-4 geomagnetic field model, *Geophys. J. Int.*, 197(2):815–827, doi:10.1093/gji/ggu033

Gillet, N., Jault, D., Finlay, C., and Olsen, N. (2013), Stochastic modelling of the earth's magnetic field: inversion for covariances over the observatory era, *Geochemistry, Geophysics, Geosystems*, 14(4):766–786, doi:10.1002/ggge.2004441

Lesur, V., Rother, M., Vervelidou, F., Hamoudi, M., and Thébault, E. (2013), Post-processing scheme for modeling the lithospheric magnetic field, *Solid Earth*, 4:105–118, doi:10.5194/sed-4-105-2013

Macmillan, S. and Olsen, N. (2013), Observatory data and the swarm mission, *Earth, Planets and Space*, 65(11):1355–1362, doi:10.5047/eps.2013.07.011

Mandea, M., Panet, I., Lesur, V., De Viron, O., Diament, M., and Le Mouël, J. L. (2012), The earth's fluid core: recent changes derived from space observations of geopotential fields, *PNAS*, doi:10.1073/pnas.1207346109

Wardinski, I. and Lesur, V. (2012), An extended version of the C^3FM geomagnetic field model - application of a continuous frozen-flux constraint, *Geophys. J. Int.*, 189:1409–1429, doi:10.1111/j.1365-246X.2012.05384.x

Geese, A., Mandea, M., Lesur, V., and Hayn, M. (2010), Regional modelling of the southern african geomagnetic field using harmonic splines, *Geophys. J. Int*, doi: 10.1111/j.1365-246X.2010.04575.x

Lesur, V., Wardinski, I., Hamoudi, M., and Rother, M. (2010), The second generation of the GFZ reference internal magnetic field model: GRIMM-2, *Earth Planets and Space*, 62(10):765–773, doi: 10.5047/eps.2010.07.007

Olsen, N., Mandea, M., Sabaka, T., and Tøffner-Clausen, L. (2010), The chaos-3 geomagnetic field model and candidates for the 11th generation igrf, *Earth Planets Space*, 62:719–727, doi:10.5047/eps.2010.07.003

Gillet, N., Lesur, V., and Olsen, N. (2009), Geomagnetic core field secular variation models, *Space. Sci. Rev.*, doi:10.1007/s11214-009-9586-6

Olsen, N., Mandea, M., Sabaka, T. J., and Tøffner-Clausen, L. (2009), CHAOS-2 – a geomagnetic field model derived from one decade of continuous satellite data, *Geophys. J. Int.*, 179(3):1477–1487, doi:10.1111/j.1365-246X.2009.04386.x

Stockmann, R., Finlay, C., and Jackson, A. (2009), Imaging earth's crustal magnetic field with satellite data: a regularized spherical triangle tessellation approach, *Geophysical Journal International*, 179(2):929–944, doi: 10.1111/j.1365-246X.2009.04345.x

Lesur, V., Wardinski, I., Rother, M., and Mandea, M. (2008), GRIMM - The GFZ Reference Internal Magnetic Model based on vector satellite and observatory data, *Geophys. J. Int.*, 173, doi:10.1111/j.1365-246X.2008.03724.x

Wessel, P. and Becker, J. (2008), Interpolation using generalized green's function for a spherical surface spline in tension, *Geophys. J. Int.*, 174:21–28, doi: 10.1111/j.1365-246X.2008.03829.x

Jackson, A., Constable, C., Walker, M., and Parker, R. (2007), Models of the Earth's main magnetic field incorporating flux and radial vorticity constraints, *Geophys. J. Int.*, 171(1):133–144, doi: 10.1111/j.1365–246X.2007.03526.x

Olsen, N., Lühr, H., Sabaka, T., Mandea, M., Rother, M., Tøffner-Clausen, L., and Choi, S. (2006), CHAOS – A model of the Earth's magnetic field derived from CHAMP, Oersted, and SAC-C magnetic satellite data, *Geophys. J. Int.*, 166(1):67–75, doi:10.1111/j.1365-246X.2006.02959.x

Whaler, K. and Purucker, M. (2005), A spatially continuous magnetization model for mars., *J. Geophys. Res.*, 110, doi:10.1029/2004JE002393

Lowes, F. J. and Olsen, N. (2004), A more realistic estimate of the variances and systematic errors in spherical harmonic geomagnetic field models, *Geophys. J. Int.*, 157:1027–1044

Whaler, K. and Langel, R. (1996), Minimal crustal magnetization from satellite data, *Phys. Earth Planet. Int.*, 48:303–319

Parker, R. L. (1994), *Geophysical Inverse Theory*, Princeton University Press, Princeton, NJ.

Constable, C. G., Parker, R. L., and Stark, P. B. (1993), Geomagnetic field models incorporating frozen-flux constraints, *Geophys. J. Int.*, 113:419–433

Shure, L., Parker, R., and Backus, G. (1982), Harmonic splines for geomagnetic modelling, *Physics of the Earth and Planetary Interiors*, 28:215–229, doi: 10.1016/0031-9201(82)90003-6

Langel, R. A., Estes, R. H., Mead, G. D., Fabiano, E. B., and Lancaster, E. R. (1980), Initial geomagnetic field model from MAGSAT vector data, *Geophys. Res. Lett.*, 7:793–796